

## Simulation of Microgrid Voltage and Current Harmonics using Coordinated Control of Dual-Interfacing-Converters

**N Santosh**

Department of Electrical and Electronics Engineering  
Gokul Institute of Technology & Science,  
Piridi, Andhra Pradesh - 535558, India.

**R.Srinivas Rao**

Department of Electrical and Electronics Engineering  
Gokul Institute of Technology & Science,  
Piridi, Andhra Pradesh - 535558, India.

### Abstract

*It is analyzed in this paper that the compensation of local load harmonic current using a single DG interfacing converter may cause the amplification of supply voltage harmonics to sensitive loads, particularly when the main grid voltage is highly distorted. The growing installation of distributed generation (DG) units in low voltage distribution systems has popularized the concept of nonlinear load harmonic current compensation using multi-functional DG interfacing converters. To address this limitation, unlike the operation of conventional unified power quality conditioners (UPQC) with seriesconverter, a new simultaneous supply voltage and grid current harmonic compensation strategy is proposed using coordinated control of two shunt interfacing converters. Specifically, the first converter is responsible for local load supply voltage harmonic suppression. To realize a simple control of parallel converters, a modified hybrid voltage and current controller is also developed in the paper. By using this proposed controller, the grid voltage phase-locked loop and the detection of the load current and the supply voltage harmonics are unnecessary for both interfacing converters. The second converter is used to mitigate the harmonic current produced by the interaction between the first interfacing converter and the local nonlinear load. Thus, the computational load of interfacing converters can be significantly reduced.*

**Index Terms**—parallel converters; active power filter; dynamic voltage restorer; LCL filter; resonance; power quality; harmonic detection; phase-locked loop.

### INTRODUCTION

There are growing demands of using power conditioning circuits [1-6] in low and medium voltage power distribution system. Comparing to bulky passive filters that are highly sensitive to circuit parameters variations, the active power conditioning equipment including active power filter (APF), dynamic voltage restorer (DVR), and unified power quality conditioner (UPQC) is preferred due the fast dynamic response and the good immunity to system parameter changes. On the other hand, the high penetration of distributed generation (DG) unit with power electronics interfacing converter offers the possibility of power distribution system harmonic current compensation using multi-functional DG interfacing converter.

Previous research mainly focused on the control of a single DG shunt interfacing converter as an APF, as their power electronics circuits have similar topology. To realize an enhanced active filtering objective, the conventional current control methods for grid-tied DG interfacing converter shall be modified. First, the wide bandwidth current controllers are used so that the frequencies of harmonic load current can fall into the bandwidth of the current controller. Alternatively, the selective frequency harmonic compensation using multi-resonant current controller has received a lot of attentions, as reported in [3] and [6]. In [9], the deadbeat controller is developed for multiple DG units with active harmonic filtering capability. In [8], the

**Cite this article as:** N Santosh & R.Srinivas Rao, "Simulation of Microgrid Voltage and Current Harmonics using Coordinated Control of Dual-Interfacing-Converters", International Journal & Magazine of Engineering, Technology, Management and Research, Volume 5 Issue 2, 2018, Page 27-33.

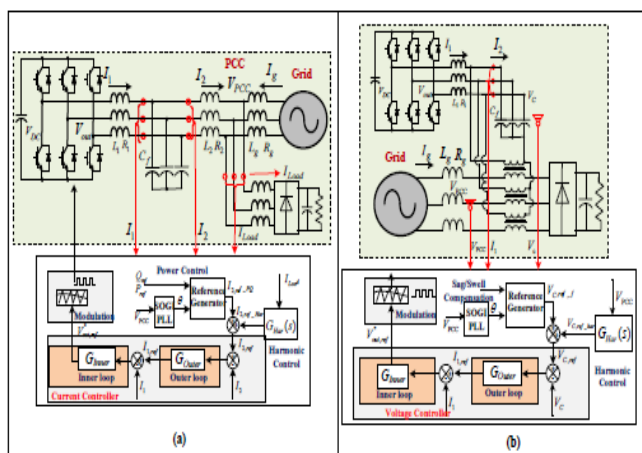
neural network method is used to improve the harmonic filtering performance of DG interfacing converters that are connected to a grid with large variation of grid impedance. In addition to the compensation of harmonics at low voltage distribution networks, the active filtering of harmonics in higher voltage distribution system using multi-level converters is discussed, as show in [7]. However, it is important to note that abovementioned compensation methods are mainly used in grid-tied converter systems. In recent literature, the hybrid voltage and current control is also developed to realize a fundamental voltage control for DG power regulation and a harmonic current control for local load harmonic compensation. Compared to the aforementioned conventional current control methods, the hybrid controller allows an interfacing converter to compensate harmonics in both grid-tied and islanding microrgrids. With assistance of the low bandwidth communications between DG units, it also possible to achieve harmonic power sharing among parallel DG systems [8].

## THE PROPOSED COORDINATED CONTROL METHOD

To have simultaneous mitigation of the supply voltage and the grid current harmonics, a compensation method using coordinated control of two parallel interfacing converters is proposed in this section. The circuitry and control diagrams of the proposed system are shown in Fig. 2 and Fig. 3, respectively. First, a DG unit with two parallel interfacing converters sharing the same DC rail is connected to PCC. Each interfacing converter has an output LCL filter and the local nonlinear load is placed at the output filter capacitor of converter1. In this topology, the supply voltage to local nonlinear load is enhanced by controlling the harmonic component of interfacing converter1. Meanwhile, the grid current harmonic is mitigated via the power conditioning through interfacing converter2. Their detailed control strategies are discussed respectively, as shown below:

### A. Control Strategy for Converter1

First, the line current  $I_{2,1}$  of converter1 and the PCC voltage  $V_{PCC}$  as shown in Fig. 2 are measured to calculate the real and reactive output power of this converter:



## II. REVIEW OF CONVENTIONAL APFAND DVR

This section briefly reviews the control of shunt APFs for grid current harmonic mitigation and series DVRs for supply voltage harmonic suppression. In order to compare with the proposed parallel-converter using modified hybrid voltage and current controller as shown in the next section, the well-understood double-loop current control and voltage control are applied to APFs and DVRs, respectively.

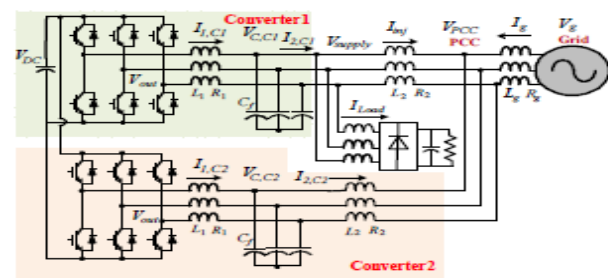
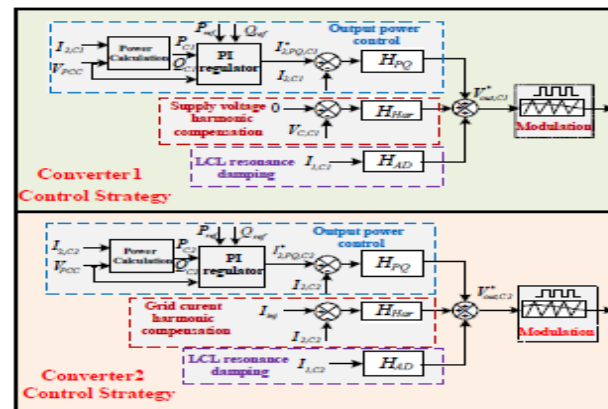


Fig. 2. Diagram of the proposed topology.



where  $PC1$  and  $QC1$  are the output real and reactive power of converter1,  $VPCC,\alpha$  and  $VPCC,\beta$  are the PCC voltage in the two-axis stationary reference frame, and  $I2\alpha,C1$  and  $I2\beta,C1$  are the line current of converter1, and  $\tau$  is the time constant of low pass filters. The time constant of the low pass filter is mainly determined by two factors. First, the real and reactive power ripples caused by line current harmonics must be properly filtered out. Secondly, the rapid dynamic power control shall be maintained. According to the design guideline in [9], the  $\tau$  is selected to be 62ms in this paper.

It is important to note that the power reference is usually determined according to the available power from the back stage of the DG unit. When there is energy storage system in the DG unit, the power reference can also be determined by the energy management system of a DG unit or a microgrid. Therefore, for the sake of simplicity, the harmonic compensation service is usually activated when there is insufficient power rating in the interfacing converters [3 and 4].

The output of the power reference generator is the line current reference  $I2,Q,C1$  as:

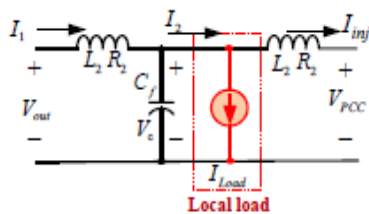
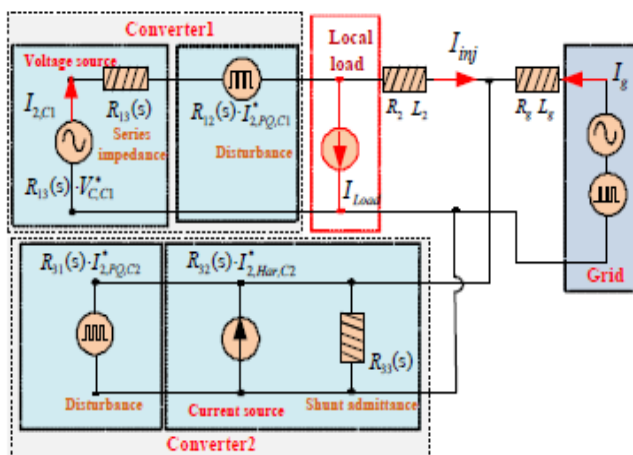


Fig. 5. Diagram of an LCL filter with a local nonlinear load.



## EVALUATION RESULTS

Simulated and experimental results are obtained to further verify the performance of the proposed controller for coordinated operation of parallel converters.

### A. Simulated results

First, similar to Fig. 1, a single interfacing converter is connected to the main grid and the local nonlinear load is placed at the output terminal of the DG unit. In this simulation, some steady-state harmonic distortion is added to the main grid voltage and the grid voltage THD is 5.6%. When the current controller as shown in (13) is applied to the system, the performance of the system is shown in Fig. 11 to Fig. 13.

As the local load harmonic current is compensated by the DG unit, it can be seen from the second channel of Fig.11 that the grid current is almost ripple-free with only 4.57% THD. On the other hand, the interfacing converter line current  $I2$  is highly distorted in this case. Due to the lack of supply voltage harmonic control, the supply voltage to the local nonlinear load is distorted with 6.45% THD.

To have a better understanding of the power quality of the system, the harmonic spectrum of the grid current and the supply voltage in Fig. 11 are given in Fig. 12 and Fig. 13, respectively.

When the supply voltage harmonic component is controlled by a single interfacing converter using the hybrid voltage and current control as shown in (9), the performance is shown in Fig. 14. As illustrated, the quality of supply voltage in this case is significantly improved with only 1.48% THD. Nevertheless, the grid current has more harmonics and the corresponding THD is 12.28%.

Similarly, the corresponding harmonic spectrum of the supply voltage and the grid current are shown in Fig. 15 and Fig. 16, respectively. Comparing to the previous spectrum analysis results in Fig. 12 and Fig. 13, it can be clearly seen that the supply voltage harmonic reduction



is achieved at the expense of more grid current distortions.

The simultaneous supply voltage and grid current harmonics mitigation is tested by using a single DG unit with two parallel interfacing converters sharing the same DC rail. The circuitry and the control strategy of the system is the same as that in Fig. 2 and Fig. 3, in which the first converter is for supply harmonics voltage reduction and the second converter is employed for harmonic current compensation.

First, the main grid voltage and the grid current are shown in Fig.17. In this case, some distortions are added to the main grid voltage and the THD is 5.7%. Due to the coordinated control of parallel converters, it can be seen that the grid current is sinusoidal with only 3.54% THD.

The performance of converter1 is shown in Fig.18. As this converter is applied to compensate the harmonics in the supply voltage, it can be seen that the voltage waveform in the top of the figure is almost ripple-free. However, the line current of this converter is distorted.

In addition, the performance of converter2 is shown in Fig.19. As the line current of converter1 produces a large amount of harmonic current, it must be properly compensated by converter2 by using the hybrid controller as shown in (13). The objective of this control strategy has been verified as the grid current is sinusoidal in the second channel of Fig.17.

To have a clear understanding of the principle of the proposed controller for parallel converter coordinated control, the spectrum of grid current and supply voltage are shown in Fig.20 and Fig.21. In this case, it can be noticed that both grid current and supply voltage quality are significantly improved.

Finally, the power control performance of the system is tested when the PQ reference has a step jump. It can be seen from Fig. 22 that both converters have a rapid response to PQ reference change. There is no obvious

overshoot during this process and the steady-state power control error is zero.

To fully verify the performance of the proposed method, a simulation is conducted where a highly distorted grid voltage with 10% THD is used, as shown in the top of Fig. 23. In this simulation, the grid voltage has 10% dip at 1.8sec. It can be clearly seen that both the supply voltage and the grid current are sinusoidal during the entire simulation. The THDs of supply voltage are 2.86% and 2.91%, before and after grid voltage dips, respectively. Similarly, the grid current THDs are 3.24% and 2.78% in these two scenarios.

### **B. Experimental results**

The proposed method is also verified on a voltage-scaled laboratory DG test rig with two parallel interfacing converters at the same power rating. The detailed circuit and control parameters can be seen from Table I and the configuration of the system is illustrated in Fig. 2.

First, only converter1 with the supply voltage harmonic mitigation as the control objective is connected to a highly distorted grid. The converter2 is disconnected from the grid in order to clearly show the characteristics of converter1

The grid voltage waveform with 7.5% THD is shown in Fig. 24. The local load in this case is a diode rectifier with the distorted current as shown in Fig. 25. Note that the distorted grid voltage and local load are used for the verification of grid current compensation and simultaneously compensation using dual-converter. As the directly supply voltage harmonic control is achieved by the second term of the controller as shown in (9), it can be noticed that the supply voltage is very smooth with only 2.01% THD. At the same time, due to a fact that the ripple-free supply voltage and the highly distorted grid voltage are interconnected with converter1 output filter choke  $L_1$ , it can be seen that both the grid current and the converter1 line current in this case have significant harmonic distortions as shown in Fig. 27 and Fig. 28, respectively.

Fig. 29 shows the power response when the active power reference increases from 0 kW to 5kW and the reactive power reference increases from 0 kVar to 5kVar. As shown, the power control reaches a steady-state for around 0.1 sec after the change of the references. In addition, it can be observed that the steady-state power control error is zero even when the supply voltage compensation is activated in the DG system.

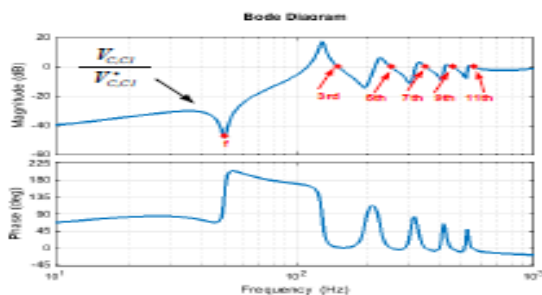


Fig. 7. Response of converter1 filter capacitor voltage  $V_{C_{C1}}$  to voltage reference  $V_{C_{C1}}$ .

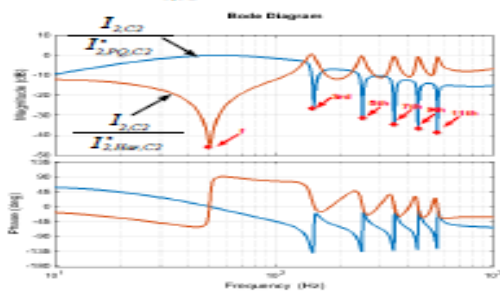


Fig. 9. Response of converter2 line current  $I_{L_{C2}}$  to power control current reference  $I_{L_{PQC2}}$  and the harmonic compensation current reference  $I_{L_{Har,C2}}$ .

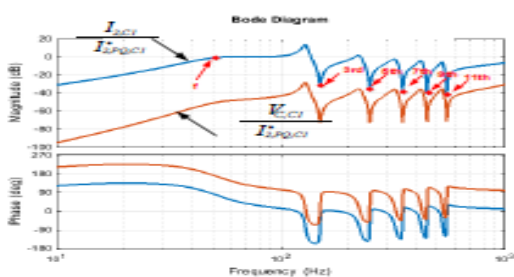


Fig. 8. Closed-loop voltage and current response of converter1 to current reference  $I_{L_{PQC1}}$ .

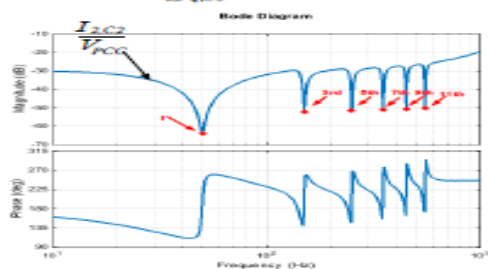
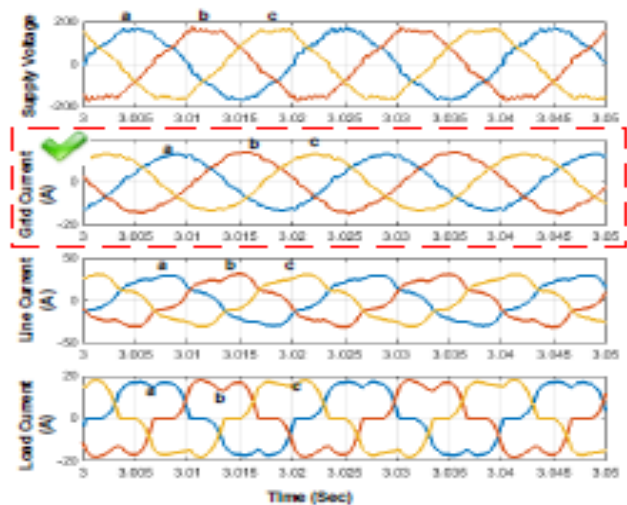


Fig. 10. Response of converter2 line current  $I_{L_{C2}}$  to PCC voltage  $V_{PCC}$ .

In addition, when only converter2 is applied to compensate the nonlinear load harmonics and the converter1 is disconnected from the grid, the corresponding performance of the system is obtained in Fig. 30 to 33. Similarly, the grid voltage is also distorted and the diode rectifier load is placed at the output of converter2, as shown in Fig. 24 and Fig. 25, respectively. However, in contrast to the counterpart as shown in Fig. 26, it can be clearly seen that the supply voltage to the local load is highly distorted in Fig. 30, with 7.3% THD. This is because the harmonic current from the local load is compensated by converter2. Thus, the three-phase grid current in this case is sinusoidal with only 4.08% as illustrated in Fig. 31. Nevertheless, since the harmonic current from the nonlinear flow to the converter2, the converter2 line current in this case has nontrivial harmonic current as shown in Fig. 32.

TABLE I. PARAMETERS OF THE SIMULATED & EXPERIMENTAL SYSTEM

Circuit Parameter	Converter1	Converter2
Rated grid voltage	Three-phase 110V/50Hz (Simulation & Experiment)	Three-phase 110V/50Hz (Simulation & Experiment)
DC link voltage	450V (Simulation & Experiment)	450V (Simulation & Experiment)
LCL filter	$L_1=1\text{mH}$ $R_1=8\text{m}\Omega$ ; $C_f=1.5\mu\text{F}$ ; $L_2=1\text{mH}$ $R_2=6\text{m}\Omega$	$L_1=1\text{mH}$ $R_1=8\text{m}\Omega$ ; $C_f=1.5\mu\text{F}$ ; $L_2=1\text{mH}$ $R_2=6\text{m}\Omega$
Sampling and Switching Frequency	20kHz/10kHz	20kHz/10kHz
Dead-time	2.25 $\mu\text{s}$	2.25 $\mu\text{s}$
Control parameter	Converter1	Converter2
Control parameters:	$k_{p1}=0.25$ ; $k_{p2}=0.25$ ; $k_{i1}=25$ ; $k_{i2}=20$ ; $k_{p3}=20$ ; $k_{p4}=20$ ; $k_{i3}=10$ ; $\omega_p=4$	$k_{p1}=0.25$ ; $k_{p2}=0.25$ ; $k_{i1}=25$ ; $k_{i2}=20$ ; $k_{p3}=20$ ; $k_{p4}=20$ ; $k_{i3}=10$ ; $\omega_p=4$

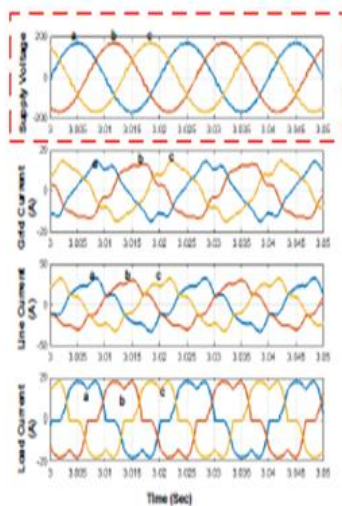


Similar to the previous test, the response to a step increase of real and reactive power reference is shown in Fig. 33. The power control characteristics in Fig. 33 are

similar to the counterpart in Fig. 29. This is because the Power Control term is very well decoupled from the Harmonic Compensation term in the proposed control method.

Up to now, the conclusion that a single shunt interfacing converter can hardly maintain improved supply voltage and grid current quality at the same time has been verified by the experimental results from Fig. 24 to Fig. 33.

When both converter1 and converter2 are connected to the experimental system to achieve simultaneous harmonic supply voltage and harmonic grid current mitigation, the corresponding is shown from Fig. 34 to Fig. 39. Similar to the previous two experiments, the grid voltage in this case is highly distorted and a nonlinear load is connected to the shunt capacitor of converter1, as shown in Fig. 24 and Fig. 25, respectively.



Only the supply voltage harmonic component is compensated. (From upper to lower:  $V_{supply}$ ,  $I_g$ ,  $I_l$ ,  $I_{load}$ )

Since converter1 is used to compensate the harmonic voltage at the local load connection point, the line current is distorted as shown in Fig. 34. As the harmonic current caused by the interactions between the local nonlinear load and the converter1 is compensated by the line current control of converter2, it can be seen from Fig. 35 that the line current of converter2 also contains significant harmonics.

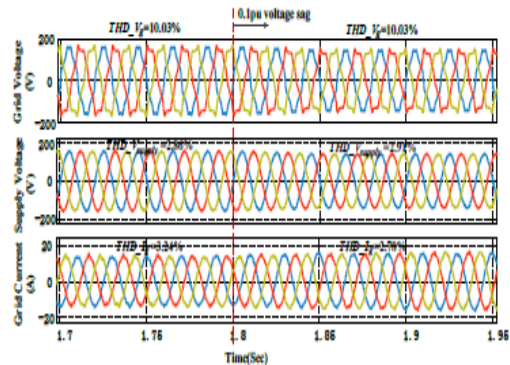


Fig. 23. The performance of the dual-converter system during 10% grid voltage sags, with 10.03% THD.

Due to the coordinated operation of both converter1 and converter2, the enhanced supply voltage and grid current quality is realized as shown in Fig. 36 and Fig. 37, respectively. The corresponding THDs of the supply voltage and the grid current are 2.25% and 3.59%, respectively. Note that during the entire process, no PLLs or harmonic extraction is involved in the control schemes. Finally, the power response of this dual-converter system is shown in Fig. 38 and Fig. 39. Due to the involvement of dual converters, the power reference for each converter is a half of that in Figs. 29 and 33. Due to the decoupled feature of the proposed method, two converters have similar response in this case and the steady-state tracking error is zero for both converters.

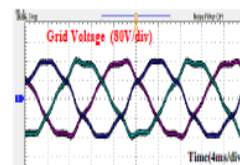


Fig. 24. Three-phase main grid voltage ( $V_g$ ).

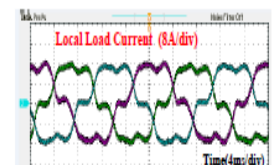


Fig. 25. Current of local load connecting to converter1 ( $I_{load}$ ).

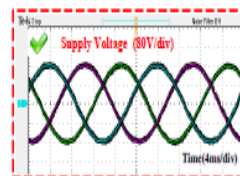


Fig. 26. Supply voltage after harmonic voltage compensation using converter1 ( $V_{supply}$ ).

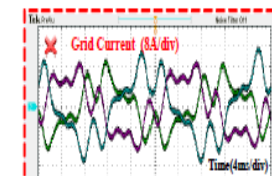


Fig. 27. Grid current ( $I_g$ ) when only converter1 is operating.

### CONCLUSION

When a single multi-functional interfacing converter is adopted to compensate the harmonic current from local nonlinear loads, the quality of supply voltage to local load can hardly be improved at the same time, particular when the main grid voltage is distorted. This paper



discusses a novel coordinated voltage and current controller for dual-converter system in which the local load is directly connected to the shunt capacitor of the first converter. With the configuration, the quality of supply voltage can be enhanced via a direct closed-loop harmonic voltage control of filter capacitor voltage. At the same time, the harmonic current caused by the nonlinear load and the first converter is compensated by the second converter. Thus, the quality of the grid current and the supply voltage are both significantly improved. To reduce the computational load of DG interfacing converter, the coordinated voltage and current control without using load current/supply voltage harmonic extractions or phase-lock loops is developed to realize coordinated control of parallel converters.

#### REFERENCES

- [1] B. Singh, K. Al-Haddad, A. Chandra, "A review of active filters for power quality improvement," *IEEE Trans. Ind. Electron.*, vol. 46, no. 5, pp. 960 - 971, May. 1999.
- [2] P. Acuna, L. Moran, M. Rivera, J. Dixon, and J. Rodriguez, "Improved active power filter performance for renewable power generation systems," *IEEE Trans. Power Electron.*, vol. 29, no.2, pp. 687-694, Feb. 2013.
- [3] Y. W. Li, F. Blaabjerg, D. M. Vilathgamuwa, and P. C. Loh, "Design and Comparison of High Performance Stationary-Frame Controllers for DVR Implementation," *IEEE Trans. Power Electron.*, vol. 22, pp. 602-612, Mar. 2007.
- [4] C. Meyer, R. W. DeDoncker, Y. W. Li, and F. Blaabjerg, "Optimized Control Strategy for a Medium-Voltage DVR – Theoretical Investigations and Experimental Results," *IEEE Trans. Power Electron.*, vol. 23, pp. 2746-2754, Nov. 2008.
- [5] F. Blaabjerg, Z. Chen, and S. B. Kjaer, "Power electronics as efficient interface in dispersed power generation systems," *IEEE Trans. Power Electron.*, vol. 19, pp. 1184-1194, Sep. 2004.
- [6] A. Timbus, M. Liserre, R. Teodorescu, P. Rodriguez, and F. Blaabjerg, "Evaluation of current controllers for distributed power generation systems," *IEEE Trans. Power Electron.*, vol. 24, no. 3, pp. 654–664, Mar. 2009.
- [7] J. M. Guerrero, L. G. Vicuna, J. Matas, M. Castilla, and J. Miret, "A wireless controller to enhance dynamic performance of parallel inverters in distributed generation systems," *IEEE Trans. Power Electron.*, vol. 19, no. 4, pp. 1205-1213, Sep, 2004.
- [8] J. M. Guerrero, J. C. Vasquez, J. Matas, L.G. de Vicuna, and M. Castilla, "Hierarchical control of droop-controlled AC and DC microgrids - A general approach toward standardization," *IEEE Trans. Ind. Electron.*, vol. 55, no. 1, pp. 158 - 172, Jan. 2011.
- [9] J. He and Y. W. Li, "Analysis, design and implementation of virtual impedance for power electronics interfaced distributed generation," *IEEE Trans. Ind. Applicat.*, vol. 47, no. 6, pp. 2525-2038, Nov/Dec. 2011.